Magnetic structure and magnetic phase transitions in $TbPtGe_2$

2001 J. Phys.: Condens. Matter 13 4471

(http://iopscience.iop.org/0953-8984/13/20/308)

INSTITUTE OF PHYSICS PUBLISHING JOURNAL OF PHYSICS: CONDENSED MATTER

J. Phys.: Condens. Matter **13** (2001) 4471–4483 www.iop.org/Journals/cm PII: S0953-8984(01)20306-3

Magnetic structure and magnetic phase transitions in $TbPtGe_2$

B Penc[1], M Hofmann[2], A Szytuła[1,4] and A Zygmunt[3]

[1] Institute of Physics, Jagiellonian University, Reymonta 4, 30-059 Kraków, Poland
[2] Berlin Neutron Scattering Centre, Hahn–Meitner Institute, D-14 100, Berlin-Wannsee, Germany
[3] W Trzebiatowski Institute for Low Temperature and Structure Research,
Polish Academy of Sciences, 50-950 Wrocław, Poland

E-mail: szytula@if.uj.edu.pl

Received 22 December 2000, in final form 5 March 2001

Abstract

Magnetic and neutron diffraction measurements have been performed on $TbPtGe_2$ at low temperatures. The compound crystallizes in the orthorhombic $YIrGe_2$-type structure (space group $Immm$); crystal structure parameters have been refined on the basis of the neutron diffraction pattern collected at $T = 30.7$ K (paramagnetic region). $TbPtGe_2$ is antiferromagnetic below $T_N = 24.2$ K. Below this temperature only one of the two Tb sublattices is ordered; the Tb magnetic moments localized at the 4(i) sites order with the simple propagation vector $\boldsymbol{k} = 0$. Below $T_{t1} = 11.4$ K the magnetic moments at the other Tb sites, 4(h), show an ordering with the propagation vector $\boldsymbol{k}_1 = [0.2677(8), 0.1312(24), 0.6989(27)]$. At $T_{t2} = 7$ K a further phase transition to a new modulated phase described by the propagation vector $\boldsymbol{k}_2 = [0.2584(5), 0, 0.5895(6)]$ is observed.

1. Introduction

This paper, concerning the magnetic properties and structure of $TbPtGe_2$, reports a part of our systematic study of the magnetic properties of $R_mT_nX_p$ ternary rare-earth intermetallic compounds, where R is a rare-earth atom, T is a d-electron atom and X is a p-electron atom. For these compounds the exchange interactions and crystalline electric field (CEF) are two factors that influence the stability of the magnetic ordering of the rare-earth magnetic moments. Competition between these two interactions leads to a large variety of magnetic structures being observed in ternary rare-earth intermetallic compounds. Because of the large interatomic distances, the exchange interactions between the localized 4f electrons are indirect and are probably mediated via the conduction electrons (Ruderman–Kittel–Kasuya–Yosida (RKKY) model). The RKKY-type exchange interactions favour long-range oscillatory-type ordering, while magnetocrystalline anisotropy connected with the CEF favours uniaxial magnetic

[4] Author to whom any correspondence should be addressed.

0953-8984/01/204471+13$30.00

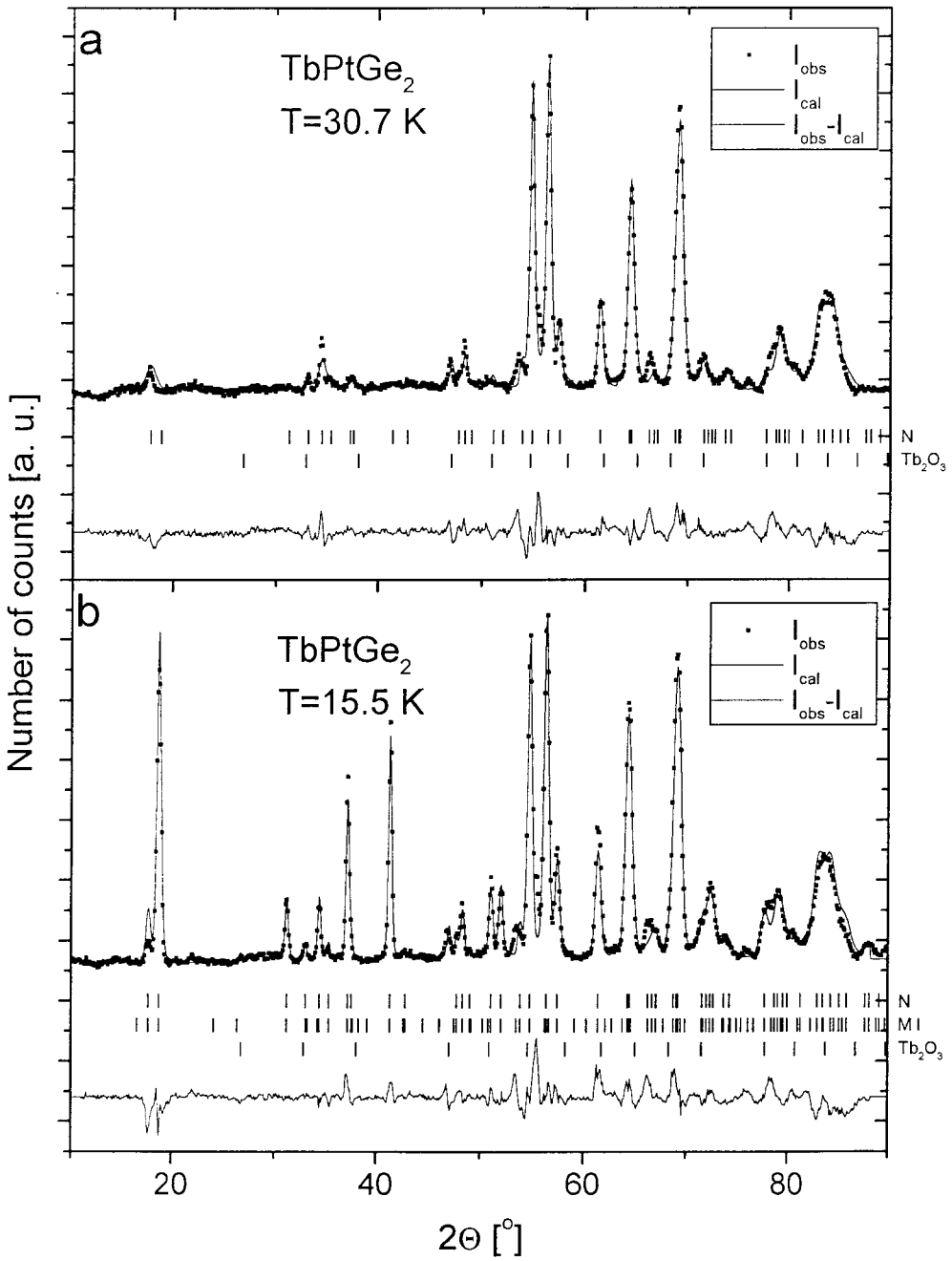

Figure 1. Neutron diffraction patterns of $TbPtGe_2$ collected at (a) 30.7 K, (b) 15.5 K, (c) 8.8 K and (d) 1.5 K. The squares represent experimental points; the solid lines are the calculated profile for the model crystal and magnetic structure as described in the text and the difference between the observed and calculated intensities (at the bottom of each diagram). The vertical bars indicate Bragg peaks of nuclear (N) and magnetic (MI—ordering in the 4(i) sublattice; MH and M′H—ordering in the 4(h) sublattice) origin for Tb_2O_3 impurity.

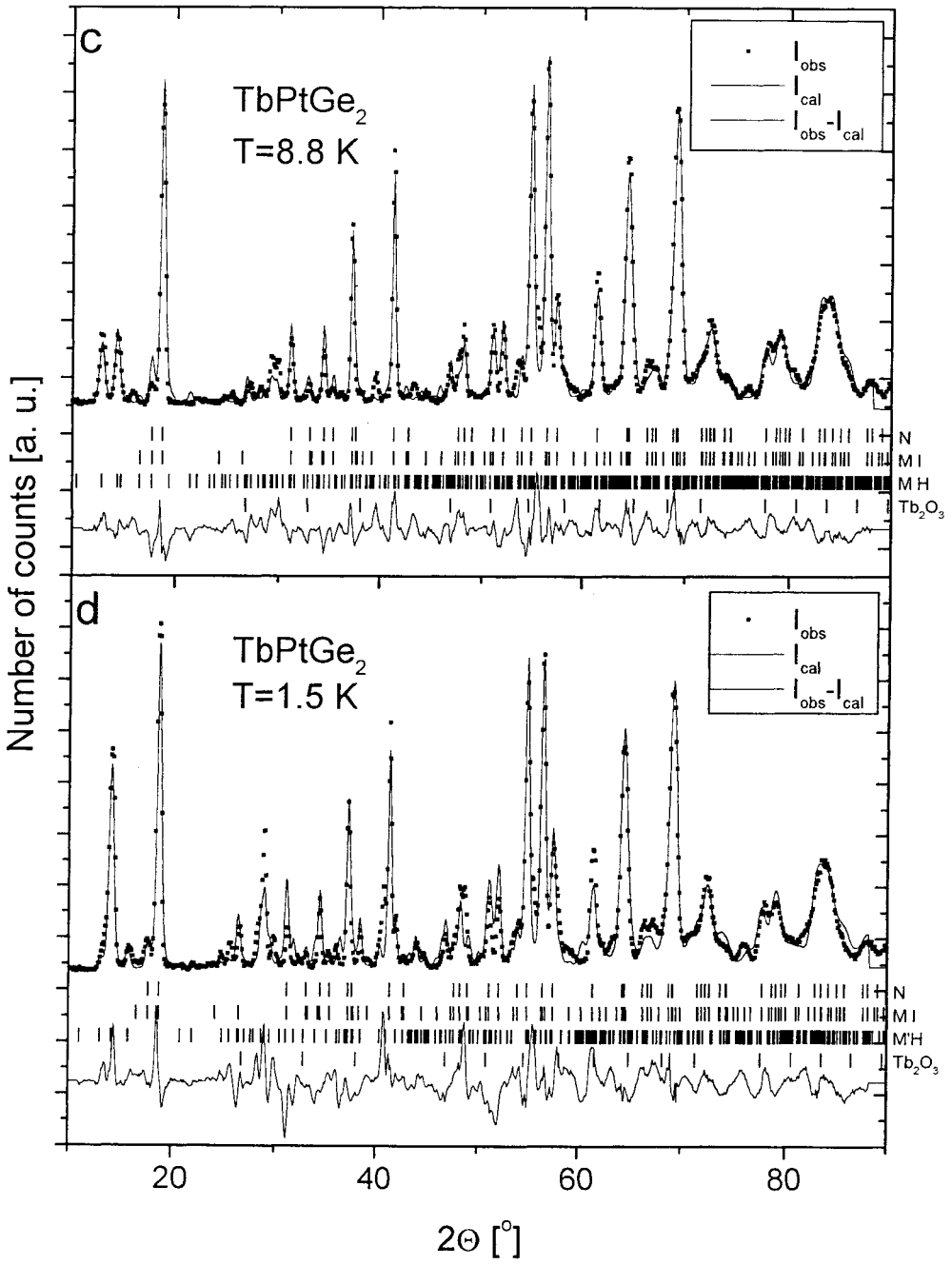

Figure 1. (Continued)

ordering. The magnetic ordering determined gives information on the role of these factors in the stability of the magnetic order. Up to now our investigations have been concentrated on compounds with three different stoichiometries: 1:1:1; 1:1:2; 1:2:2 in which the rare-earth atoms occupy only one crystallographic position in the crystal unit cell. The magnetic

data concerning these compounds are summarized in the books [1, 2]. We have now started investigations on compounds with more complicated crystal structure. The $RPtGe_2$ family of compounds crystallize in the orthorhombic $YIrGe_2$-type structure [3]. In this structure the rare-earth atoms occupy two nonequivalent crystallographic positions of very low symmetry. In such a case the spin–orbit coupling and the magnetocrystalline anisotropy play significant roles and influence the magnetic properties of compounds. The above-mentioned compounds are also good subjects for investigation of the influence of the crystal structure on magnetic properties. Magnetic properties have been investigated only for some of these compounds. The $RPtGe_2$ compounds with Dy and Ho exhibit antiferromagnetic ordering at low temperatures [4, 5]. Neutron diffraction data for $DyPtGe_2$ indicate two magnetic phase transitions: at 14 K and 5 K. At $T_N = 14$ K the change from the paramagnetic state to the incommensurate antiferromagnetic structure with the propagation vector $\boldsymbol{k}_1 = (0.495, 0, 0)$ is observed. At 5 K the propagation vector changes into $\boldsymbol{k}_2 = (0.268, 0, 0)$ and the amplitude-sine-wave-modulated structure changes from one of nearly transverse type to one of longitudinal type. The ordered moments are 8.5 μ_B and 9.9 μ_B at 8 K and 4 K, respectively [4]. $HoPtGe_2$ has commensurate antiferromagnetic structure with the propagation vector $\boldsymbol{k} = 0$. At 4 K the ordered Ho moments are 8.1 μ_B at the 4(i) sites and 4.0 μ_B at the 4(h) sites with their directions lying in the a–b and the b–c planes, respectively [5].

This paper reports the results of magnetic and neutron diffraction measurements which have been carried out to determine the magnetic properties and the crystal and magnetic structure of $TbPtGe_2$.

2. Experimental procedure

The polycrystalline $TbPtGe_2$ sample was synthesized by arc melting stoichiometric amounts of high-purity Tb, Pt and Ge elements. The sample was annealed in an evacuated quartz tube at 1200 K for one week.

In order to check the purity of the sample obtained, it was examined by means of x-ray powder diffraction. The results reveal that the sample is single phase with a small amount of Tb_2O_3. The analysis of the composition by the EDAX method gives the stoichiometry $Tb_{1.01}Pt_{1.00}Ge_{1.95}$.

Magnetic susceptibility and magnetization data were collected using a vibrating-sample magnetometer and a SQUID magnetometer in the temperature range from 2 to 300 K and in external magnetic fields up to 50 kOe.

Neutron diffraction patterns were obtained on the E6 instrument at the BER II reactor (Hahn–Meitner Institute, Berlin). The incident neutron wavelength was 2.412 Å. Diffraction patterns were recorded at different temperatures between 1.5 and 30.7 K. The Rietveld-type program Fullprof [6] was used for processing the neutron diffraction data. Neutron scattering length values were taken from reference [7]; the form factor for the Tb^{3+} ion was calculated after reference [8].

3. Results

3.1. Crystal structure

The neutron diffraction pattern recorded in the paramagnetic state at 30.7 K (figure 1(a)) confirmed that $TbPtGe_2$ has the orthorhombic crystal structure of the $YIrGe_2$ type. A small fraction ($\lesssim 3\%$) of Tb_2O_3 can be discerned in the diffraction pattern shown in figure 1(a) but all of the main observed reflections are indexed according to the space group $Immm$. The unit

cell contains eight formula units. The atoms occupy the following positions: Tb(1) 4(i) site: $(0, 0, z)$; Tb(2) 4(h) site: $(0, y, \frac{1}{2})$; Pt 8(l) site: $(0, y, z)$; Ge(1) 4(h) site: $(0, y, \frac{1}{2})$; Ge(2) 4(g) site: $(0, y, 0)$; and Ge(3) 8(l) site: $(0, y, z)$ (see figure 2). The values of the lattice parameters a, b and c as well as the positional parameters corresponding to the minimum of the reliability factor are listed in table 1.

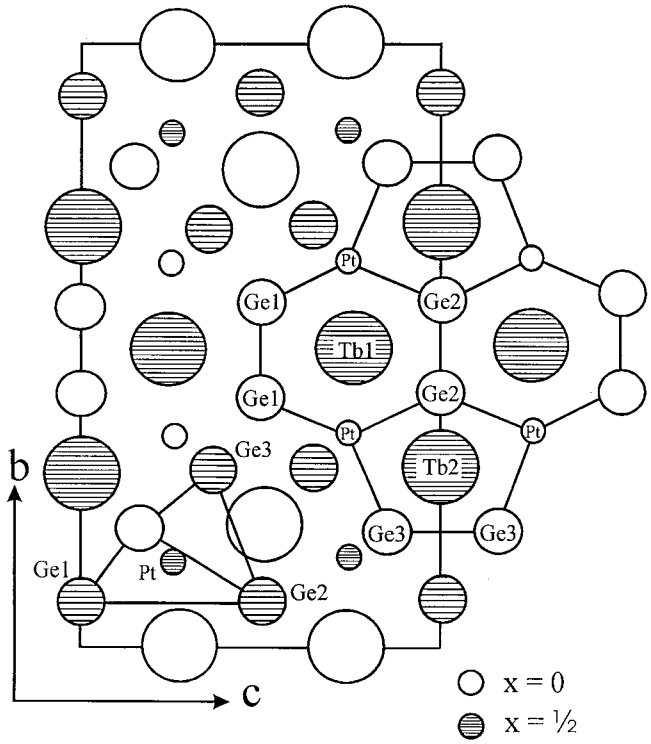

Figure 2. The projection of the $TbPtGe_2$ unit cell onto the (100) plane.

Table 1. The refined structural parameters of $TbPtGe_2$ at $T = 30.7$ K (space group $Immm$ (No 71)); standard deviations are given in parentheses.

Atom	Position	x	y	z
Tb(1)	4(i)	0.0	0.0	0.2480(30)
Tb(2)	4(h)	0.0	0.1926(17)	0.5
Pt	8(l)	0.0	0.1497(6)	0.2556(15)
Ge(1)	4(h)	0.0	0.0748(17)	0.5
Ge(2)	4(g)	0.0	0.0868(14)	0.0
Ge(3)	8(l)	0.0	0.2983(12)	0.3531(15)

$a = 4.3338(17)$ Å
$b = 16.3207(78)$ Å
$c = 8.7170(36)$ Å

$R_{Bragg} = 8.8\%$
$R_{prof} = 7.1\%$
$R_{exp} = 2.8\%$

3.2. Magnetic data

3.2.1. Magnetometric measurements. The temperature dependence of the magnetization at low magnetic fields (100 and 200 Oe) shows a very small anomaly at 24.2 K and three additional features at 11.4, 7.0 and 2.45 K (figure 3(a)). These anomalies are also visible in external magnetic fields up to 50 kOe. In the latter case a small decrease in the transition temperatures with increasing magnetic field is observed (figure 3(b)). The anomaly at 2.45 K corresponds to the Néel temperature of the impurity Tb_2O_3 [9].

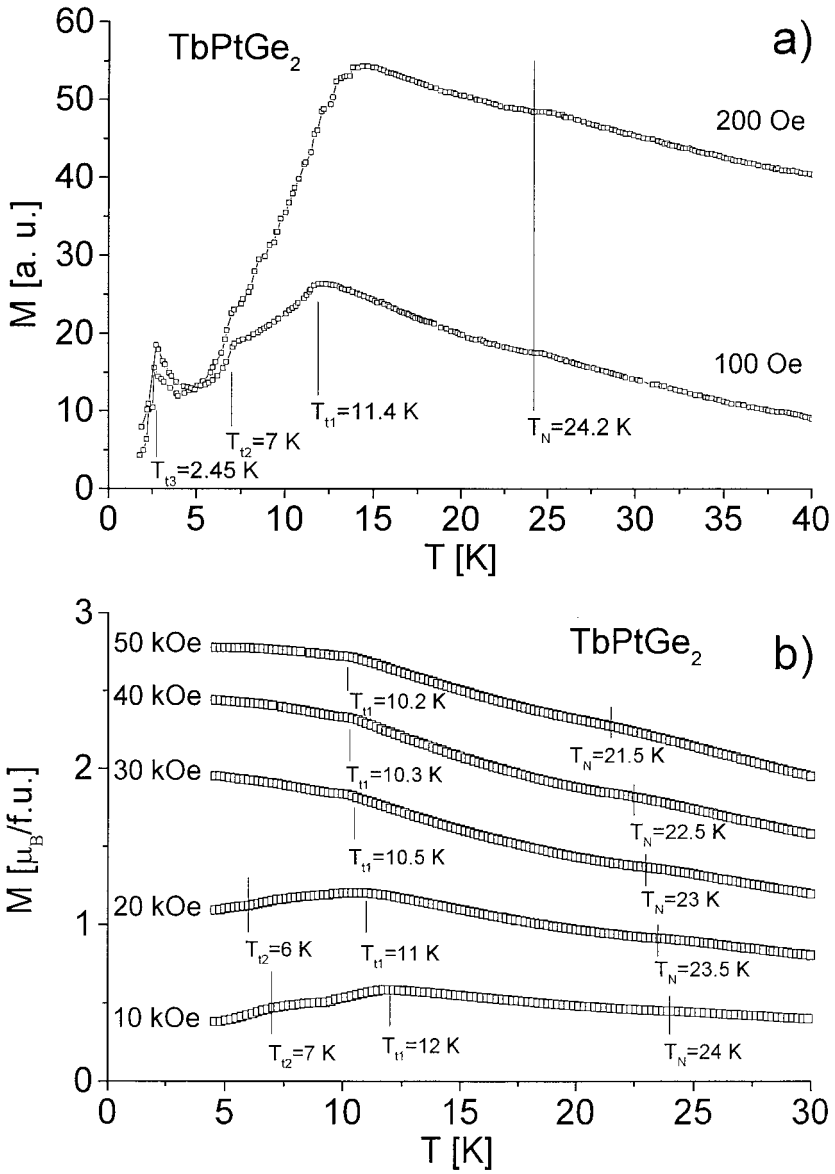

Figure 3. The temperature dependence of the magnetization of $TbPtGe_2$ at low (a) and high (b) magnetic fields. The anomaly observed at T_{t3} corresponds to the Néel temperature of Tb_2O_3.

The magnetization curve $M(H)$ at 4.2 K indicates the existence of metamagnetic transitions in $TbPtGe_2$ (figure 4(a)). The values of the critical fields were determined from the plot of the differential magnetization against the external magnetic field (figure 4(b)). Because our measurements were performed on the polycrystalline sample, the transition does not occur abruptly at a well-defined field but lasts over a range of field values and appropriate average values are 12.5 and 22 kOe, respectively. The magnetization curve measured for the increasing and then decreasing magnetic field shows a small hysteresis (figure 4(a)). The magnetic moment determined at 4.2 K and $H = 50$ kOe is equal to 2.7 μ_B/f.u. and is much smaller

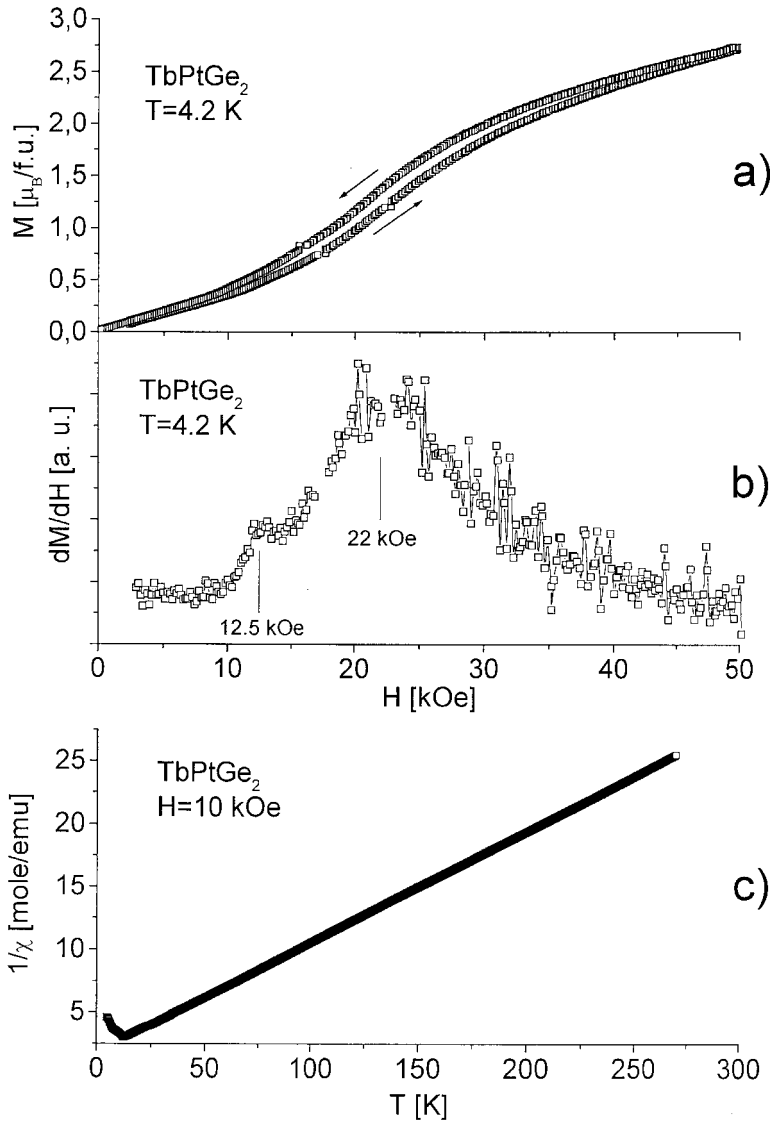

Figure 4. (a) The field dependence of the magnetization of $TbPtGe_2$ at 4.2 K. The arrows show the directions of the changes of the external field during the measurement. (b) The differential magnetization of $TbPtGe_2$ versus the external magnetic field. (c) The temperature dependence of the reciprocal magnetic susceptibility of $TbPtGe_2$.

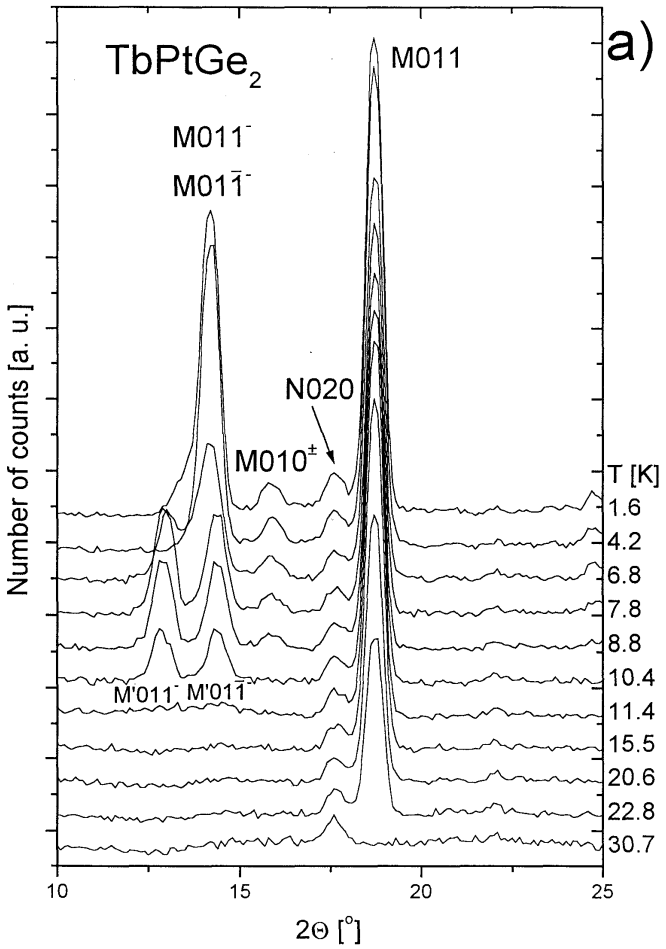

Figure 5. (a) Neutron diffraction patterns of $TbPtGe_2$ in the 2θ-range from 10° to 25° collected at several temperatures between 1.5 K and 30.7 K. (b) The thermal variation of the intensities of the magnetic peaks characteristic for magnetic ordering at the 4(i) (M011) and 4(h) sites ($M011^-$ and $M01\bar{1}^-$).

than the respective free-Tb^{3+}-ion value (9.72 μ_B). More precise and exact analysis of the magnetization curve requires new measurements on a single crystal.

Above 30 K the reciprocal magnetic susceptibility obeys the Curie–Weiss law with the paramagnetic Curie temperature equal to 20 K and the effective magnetic moment of 9.54 μ_B/Tb atom (figure 4(c)), which is approximately the free-Tb^{3+}-ion value (9.72 μ_B).

3.2.2. Magnetic structure. The diffraction patterns of $TbPtGe_2$ for 2θ ranging from 10° to 25° and for temperatures between 1.6 and 30.7 K are collected in figure 5(a). In this 2θ-range only one nuclear peak (N020) is observed at 30.7 K while at 22.8 K the new peak of magnetic origin (M011) appears and at 10.4 K some additional peaks of magnetic origin are visible. In figure 5(b) the temperature dependences of the intensities of some of the magnetic peaks shown in figure 5(a) are presented. The change in the intensity of these peaks is clearly visible. Below $T_N = 24.2$ K the intensity of the (011) peak ($2\theta = 18.7^\circ$) increases and below $T_t = 11.4$ K

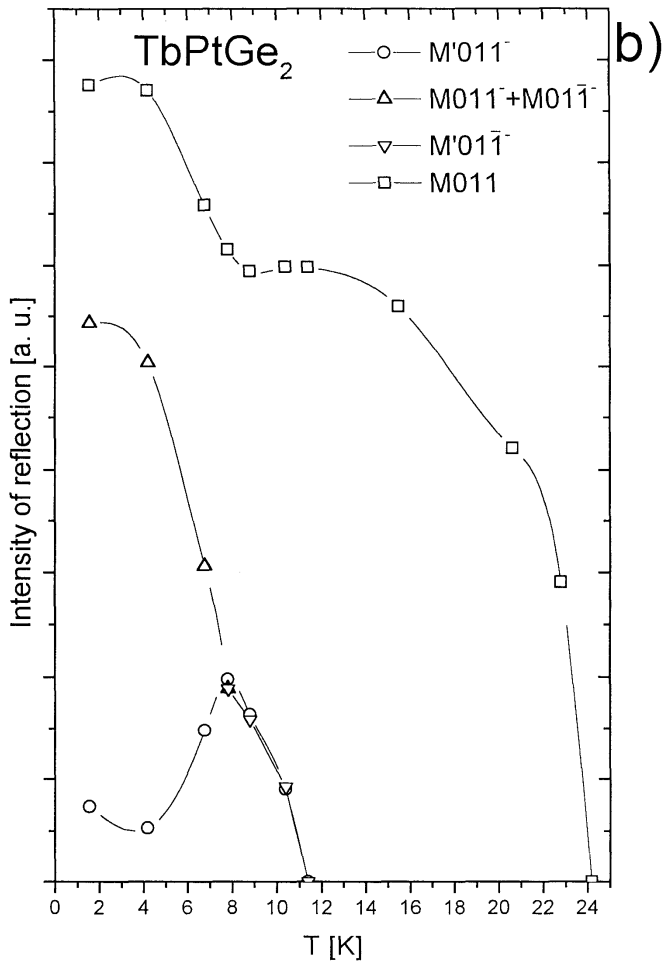

Figure 5. (Continued)

some new peaks are observed. At 9.0 K a jump in the intensity of the (011) peak is observed. The intensities and positions of the magnetic peaks change with decreasing temperature. This indicates the change of the magnetic structure with temperature that is discussed below.

All of the peaks in the neutron diffraction pattern collected at 15 K (figure 1(b)) could be indexed as ones for the $YIrGe_2$-type structure ($h + k + l = 2n$). The Rietveld-type line profile analysis indicates a significant contribution of magnetic origin to the intensity of each reflection. The best refinement (reliability factor $R_{mag1} = 9.9\%$) was obtained for the following magnetic structure (figure 6(a)):

- The terbium magnetic moment in the 4(i) sublattice occupies the following positions in the crystal unit cell: $\boldsymbol{\mu}_1(0, 0, z_1)$, $\boldsymbol{\mu}_2(0, 0, \bar{z})$, $\boldsymbol{\mu}_3(\frac{1}{2}, \frac{1}{2}, \frac{1}{2} + z_1)$ and $\boldsymbol{\mu}_4(\frac{1}{2}, \frac{1}{2}, \frac{1}{2} - z_1)$. They form an antiferromagnetic arrangement with the orientation of magnetic moments as follows: $\boldsymbol{\mu}_1 - \boldsymbol{\mu}_2 + \boldsymbol{\mu}_3 - \boldsymbol{\mu}_4$. The Tb moment is equal to 7.52(11) μ_B and is parallel to the b-axis ($R_{mag1} = 9.9\%$),
- The terbium magnetic moments at the 4(h) sites are not ordered.
- No magnetic moment is detected on platinum within the accuracy of the experiment.

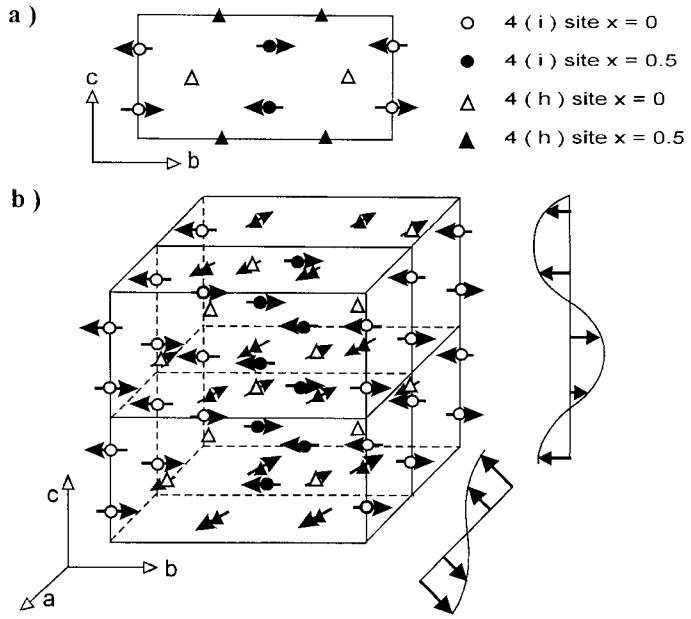

Figure 6. The magnetic structure of $TbPtGe_2$ at 15.5 K (a) and 1.5 K (b).

Several peaks are observed in the 8.8 K diffraction pattern (figure 1(c)) additional to those obtained in the 15 K pattern (figure 1(b)). These peaks could be indexed and a satisfactory refinement is obtained for the following model:

- the terbium moments at the 4(i) sites form the same structure as was found at 15 K; the magnetic moment is equal 7.84(15) μ_B (reliability factor $R_{mag1} = 9.1\%$).
- The terbium moments at the 4(h) sites form a sine-wave-modulated structure with the propagation vector $\boldsymbol{k}_1 = [0.2677(8), 0.1312(24), 0.6989(27)]$; they form an antiferromagnetic arrangement with the orientation of the magnetic moments $\boldsymbol{\mu}_1 - \boldsymbol{\mu}_2 - \boldsymbol{\mu}_3 + \boldsymbol{\mu}_4$ in the crystal unit cell. The magnetic moment equals 6.70(22) μ_B and lies in the b–c plane forming an angle of 13.5° with the c-axis ($R_{mag2} = 17.3\%$).

A different distribution of the peaks corresponding to the modulated structure is observed in the diffraction pattern at 1.5 K (figure 1(d)). The analysis of all of the peaks in this pattern leads to the following model of the magnetic structure:

- The Tb moments localized at the 4(i) sites form the above-described structure with the magnetic moment equal 8.07(1) μ_B ($R_{mag1} = 7.4\%$),
- the Tb moments localized at the 4(h) sites form the new sine-wave-modulated magnetic structure that could be described on the basis of the propagation vector $\boldsymbol{k}_2 = [0.2584(5), 0, 0.5895(6)]$. The Tb magnetic moment equals 9.0(2) μ_B and lies in the a–b plane forming an angle of 48° with the b-axis ($R_{mag2} = 11.8\%$). There are also observed peaks of small intensities, corresponding to the magnetic structure determined by the propagation vector $\boldsymbol{k}_1$.

Schematic diagrams of the magnetic structure of $TbPtGe_2$ at 15.5 K (a) and at 1.5 K (b) are shown in figure 6.

In table 2 the reliability factors of the adjustments of the crystal and magnetic structures at different temperatures are collected.

Table 2. Values of the reliability factors for $TbPtGe_2$.

T (K)	R_{exp} (%)	R_{Bragg} (%)	R_{prof} (%)	R_{mag1} (%)	R_{mag2} (%)
3.7	2.8	8.8	7.1	—	—
15.5	2.7	9.8	6.2	9.9	—
8.8	2.8	6.8	4.5	9.1	17.3
1.5	2.7	8.0	6.3	7.4	11.8

4. Discussion

The neutron diffraction data confirm that $TbPtGe_2$ crystallizes in the orthorhombic $YIrGe_2$-type structure. The atomic coordinates determined are similar to those of the isostructural compounds $DyPtGe_2$ and $HoPtGe_2$ [4, 5]. The projection of the unit cell onto the (100) plane and the coordinations of the atoms are shown in figure 2. The Tb atoms occupy two non-equivalent crystallographic positions of the same symmetry (mm) but with different atomic surroundings: four Pt and eight Ge atoms for the 4(i) site and four Pt and six Ge atoms for the 4(h) site.

The results presented in this work indicate the complex character of the magnetic order in $TbPtGe_2$. The magnetic and neutron diffraction data indicate that $TbPtGe_2$ is antiferromagnetic below $T_N = 24.2$ K. Below this temperature only the Tb magnetic moments in the 4(i) sublattice order and form a collinear antiferromagnetic structure. The 4(h) sublattice remains not ordered down to $T_{t1} = 11.4$ K where it forms a sine-wave-modulated structure with further reordering at $T_{t2} = 7$ K where the propagation vector changes. No changes in the ordering of the 4(i) sublattice are observed at T_{t1} and T_{t2}.

Similar properties were reported for isostructural $TbPdGe_2$ [10] and $TbIrGe_2$ [11]. For $TbPdGe_2$ it was found that below $T_N = 28$ K the Tb magnetic moments localized at the 4(i) sites order with the simple propagation vector $\boldsymbol{k} = 0$ and below 6.5 K the Tb moments localized at the 4(h) sites order with the propagation vector $\boldsymbol{k} = (0, \frac{1}{2}, \frac{1}{2})$. In the case of the compound $TbIrGe_2$, below $T_N = 10.2$ K the Tb magnetic moments localized at the 4(i) sites order with the simple propagation vector $\boldsymbol{k} = 0$ and below 9.0 K the Tb moments localized at the 4(h) sites order with the propagation vector $\boldsymbol{k} = (\frac{1}{2}, \frac{1}{2}, 0)$. All three compounds, i.e. $TbPtGe_2$, $TbPdGe_2$ and $TbIrGe_2$, have similar magnetic structures, as long as one is considering the Tb magnetic moments at the 4(i) sites. At low temperatures $TbPdGe_2$ and $TbIrGe_2$ have commensurate magnetic structures with the Tb magnetic moments localized at the 4(h) sites, while in the case of $TbPtGe_2$ two incommensurate structures stable in two different temperature regions were observed. These results confirm that the magnetic interactions between magnetic moments in the 4(i) sublattice are predominant and lead to a collinear antiferromagnetic ordering restricted to just this sublattice.

The coupling between the magnetic moments within the 4(h) sublattice seems to be weaker than that in the 4(i) one, as the 4(h) sublattice orders at lower temperatures than the 4(i) sublattice. The fact that the 4(i) sublattice orders antiferromagnetically leads to the extinction of the contribution to the exchange fields on the 4(h) sites arising from the 4(i) sublattice. This could explain why the 4(h) sublattice does not order magnetically in the high-temperature phase. The Tb magnetic moments in the 4(h) sublattice order at $T_{t1} = 11.4$ K. Below this temperature a sharp increase in the intensity of the magnetic M011 reflection ($2\theta = 18.7^\circ$), corresponding to the magnetic order of the Tb moments localized at the 4(i) sites, is observed (figure 5(b), open squares). This indicates the interactions between Tb magnetic moments in two distinct magnetic sublattices, i.e. 4(h) and 4(i).

Following Hutchings' notation [12], the CEF Hamiltonian for the $J = 6$ ion with the orthorhombic point symmetry is given by

$$H = B_2^0 O_2^0 + B_2^2 O_2^2 + B_4^0 O_4^0 + B_4^2 O_4^2 + B_4^4 O_4^4$$

where B_n^m and O_n^m are the CEF parameters and Stevens operators, respectively. For the compounds studied the B_2^0-coefficient is dominant since the others are smaller by an order of magnitude. The direction of the lanthanide magnetic moment is correlated with the sign of the B_2^0-coefficient in the CEF Hamiltonian: the negative sign of the B_2^0-parameter implies that the magnetic moment is directed along the *b*-axis, whereas its positive sign is correlated with the moment lying in the *a*–*c* plane [13].

In the $TbTGe_2$ (T = Pd, Pt, Ir) compounds the Tb magnetic moments at the 4(i) sites are parallel to the *b*-axis, which suggests that the B_2^0-parameter is negative. The case of Tb moments at the 4(h) sites is different: only in $TbPdGe_2$ are they parallel to the *b*-axis, while in $TbIrGe_2$ they lie in the *a*–*c* plane and in $TbPtGe_2$ in the *a*–*b* plane. These results indicate the different values of the B_n^m-parameters for the Tb ions at the 4(h) sites and the change of these parameters with the change of the T element.

The significance of the CEF effects is also visible in the results obtained for other $RPtGe_2$ compounds:

- In $DyPtGe_2$ at 5 K the amplitude-sine-wave-modulated structure changes from one of nearly transverse type to one of longitudinal type [4].
- In $HoPtGe_2$ the holmium moments located at different crystallographic positions have different orientations: lying in the *b*–*c* plane at the 4(i) sites and in the *a*–*b* plane at the 4(h) sites [5].

The above-mentioned results, along with those presented in this work for $TbPtGe_2$, indicate that the B_2^0-parameter changes with increasing number of 4f electrons. Similar properties are observed in many series of lanthanide intermetallic compounds [1].

5. Conclusions

The neutron diffraction data show that the ternary terbium compound $TbPtGe_2$ crystallizes in the orthorhombic $YIrGe_2$-type structure (space group $Immm$). The results obtained in this work indicate that the two Tb sublattices order antiferromagnetically at low temperatures: at 24.2 K only the Tb magnetic moments at 4(i) sites order and at 11.4 K the 4(h) sublattice orders. Below 11.4 K a small interaction between Tb moments is observed in both sublattices.

The Tb moments at the 4(i) sites form the simple collinear antiferromagnetic structure determined by the propagation vector $\boldsymbol{k} = 0$. This order is stable in the temperature range up to $T_N = 24.2$ K. Below $T_{t1} = 11.4$ K the Tb moments at the 4(h) sites form the sine-wave-modulated structure determined by the propagation vector $\boldsymbol{k}_1 = [0.2677(8), 0.1312(24), 0.6089(27)]$. With decreasing temperature the change of the propagation vector to $\boldsymbol{k}_2 = [0.2584(5), 0, 0.5895(6)]$ takes place and the change of the direction of the magnetic moment from the *b*–*c* plane to the *a*–*b* plane is observed. The above results indicate that $TbPtGe_2$ and the isostructural compounds $TbPdGe_2$ [10] and $TbIrGe_2$ [11] belong to the new group of compounds in which the Tb moments at different crystal sites order at different temperatures. The data concerning the directions of the magnetic moments of $DyPtGe_2$ [4] and $HoPtGe_2$ [5] and of the above-mentioned Tb compounds suggest that the magnetocrystalline anisotropy connected with the crystal electric field plays the dominant role.

Acknowledgments

This work was supported by the European Commission under the Access to Research Infrastructures of the Human Potential Programme (contract number HPRI-CT-1999-00020). The authors (BP and AS) would like to express their gratitude to the management of the Berlin Neutron Scattering Centre for financial support and kind hospitality.

The authors are greatly indebted to Dr T Jaworska-Gołąb for discussing many details of this work.

References

[1] Szytuła A and Leciejewicz J 1994 *Handbook of Crystal Structures and Magnetic Properties of Rare Earth Intermetallics* (Boca Raton, FL: Chemical Rubber Company Press)
[2] Szytuła A 1999 *Crystal Structures and Magnetic Properties of RTX Rare Earth Intermetallics* (Kraków: Wydawnictwo Uniwersytetu Jagiellońskiego)
[3] Francois M, Venturini G, McRae E, Malaman B and Roques B 1987 *J. Less-Common Met.* **128** 249
[4] Papathanassiou G, Kotsanidis P A, Yakinthos J K and Schäfer W 1998 *Z. Kristallogr.* **213** 28
[5] Papathanassiou G, Kotsanidis P A, Yakinthos J K and Schäfer W 1999 *J. Alloys Compounds* **290** 17
[6] Rodriguez-Carvajal J 1993 *Physica* B **192** 55
[7] Sears V G 1992 *Neutron News* **3** 26
[8] Freeman A J and Desclaux J P 1979 *J. Magn. Magn. Mater.* **12** 11
[9] MacChesney J B, Williams H J, Sherwood R C and Potter J F 1966 *J. Chem. Phys.* **44** 596
[10] Schmitt D, Ouladdiaf B, Routs Ch D, Yakinthos J K and Gamari-Seale H 1999 *J. Alloys Compounds* **292** 21
[11] Gil A, Szytuła A, Penc B and Hofmann M 2001 to be published
[12] Hutchings N T 1964 *Solid State Physics* vol 16 (New York: Academic) p 227
[13] Nguyen V N, Rossat-Mignod J and Tchéou F 1975 *Solid State Commun.* **17** 101